POLITECNICO DI TORINO
Repository ISTITUZIONALE

Tunable Frequency Selective Surface Design Using Automated Random Optimization

(Article begins on next page)

19 May 2024

Tunable Frequency Selective Surface Design Using Automated Random Optimization

Farzad Mir[1+], Lida Kouhalvandi[2+*], and Ladislau Matekovits[3+◇#]

[+]Department of Electronics and Telecommunications, Politecnico di Torino, Turin, Italy
[*]Department of Electronics and Communication Engineering, Istanbul Technical University, Istanbul, Turkey
[◇]Department of Measurements and Optical Electronics, Politehnica University Timisoara, Romania
[#]National Research Council of Italy, 10129 Turin, Italy
farzad.mir@studenti.polito.it [1], kouhalvandi@itu.edu.tr [2], ladislau.matekovits@polito.it [3]

Abstract

We present an automated approach to design a high performance, tunable frequency selective surface (FSS). The main goal of this study is to provide the *simultaneous* optimization of the FSS structure in two states of the 4 incorporated varactors, aiming to get an acceptable polarization filtering and polarization control. Generally, microwave designs are dealing with a large amount of data and they depend on the engineer's experiences. In order to get rid of this dependency and providing a ready-to-fabricate layout, we propose an optimization-oriented method based on the random optimization (RO). The RO method is applied in an automated environment where HFSS and Matlab are collaborating together forming a co-simulation platform where the design parameters are optimized up to achieve suitable output performances.

1 Introduction and motivation

Frequency selective surfaces (FSSs) are usually made of an identical geometrical entity, called unit-cell; illuminated by an incident field, they act as filters, polarization converters, or exhibit other interesting features. FSSs can be widely used in various applications such as a cover for satellites, radomes, microwave stoves, etc.

The *passive* configurations have been widely used in the past, but recently *tunable* versions have received a more considerable attention [1] due to the possibility of real-time control of the transmission/reflection of the incident electromagnetic wave. Such feature can be efficiently exploited in many applications, from security to sensing, etc. The *dynamic*, tunable, counterpart incorporates active devices, that requires biasing for their tunability. The presence of the active elements inserts losses, while the existence of the biasing network makes the structure more complex with respect to the relatively simple construction of the passive arrangement. The increased complexity that represents additional degrees of freedom has a controversial double effect on the design: on one hand it allows control of the structure's response, while on the other hand it makes the design more complex.

Due to the complexity of the microwave designs, optimization techniques can be employed to reduce it [2–6]. Recently, for designing FSSs, various optimization methods have been considered. Particle swarm optimization, distribution algorithm, gradient optimization algorithm, and ant colony optimization technique [7–12] are just few of them. These methods are successful algorithms in designs circuits but the outcome also depends on the designer's experience since the optimization process is under their control and supervision. To avoid the subjectivity arisen due to this aspect, we see the need of providing a study where optimization is employed in an automated environment with a combination of numerical analyzer and electronic design automation (EDA) tools. The EDA tools such as HFSS, ADS, AWR, etc. are some of the commercially available tools in the design in the microwave field. However, when a huge amount of data is to be considered for optimization, the use of external codes can be considered, since they allow a more direct access to the data. Among the possible platforms that can be used to implement independent optimizer one is Matlab.

In this work, we present the design and implementation of FSS structure with the Random Optimization (RO) where the dimensions of the geometry of the FSS are achieved automatically. Importantly, as all the process is performing automatically, there is no human interruption in the optimization of the shape of the FSS. The automated environment is created using two commercial software, namely HFSS and Matlab. The result is the high performance FSS design with acceptable and suitable properties. Hence, without any dependency to any designer's experience, the ready-to-fabricate layout can be generated.

The initial design of FSS is created by providing two circular ring resonators with different radius dimensions. Two orthogonal microstrip lines parallel to the edges of the unit cell are then added to the structure and connect the two rings and intersect in

the center. In order to tune the designed FSS, three via-holes are considered which are connected to the biasing lines that are located below the main structure described above. The biasing network consists of other two microstrip lines embedded in the dielectric supporting the main structure. They are parallel to the two microstrip lines of the main structure and are located at different levels (at a distance of 0.8 mm and symmetrically with respect to the middle of the dielectric layer) to avoid short circuit between them. Their role is to bias some diodes located within the main structure. The redundancy of the via-holes aims to avoid symmetry-breaking of the structure. A computer-aided design (CAD) model of the structure is reported in Fig. 1.
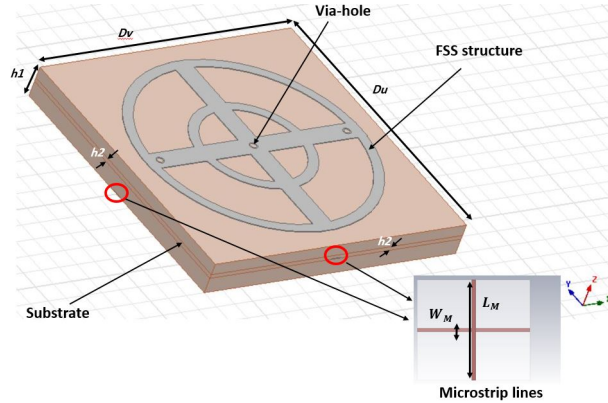

Figure 1. Geometry of the initial unit cell with the leading dimensions

In this paper, tunability is implemented by incorporating diodes in the main structure. To do so, the structure has to be modified in such a way to incorporate these lumped elements. In particular, we considered 4 slots in the main structure that will accommodate as many varactors to be identically biased. These slots are located along the radially running microstrip lines and in between the two ring resonators.

Using diodes in the slots will provide them with two main conditions: (*i*) open circuit and (*ii*) short circuit, respectively. The open circuit condition corresponds to low voltage, and is equivalent to a capacitor. Contrarily, the short-circuit configuration is the model for small values of resistor at high biasing voltage. These two states are schematically represented in Fig. 2. Using an appropriate model, it has been recently demonstrated [13] that the presence of the diodes in the two working conditions mentioned above gives similar responses as for the non-loaded main structure and for the non-loaded structure with cuts.
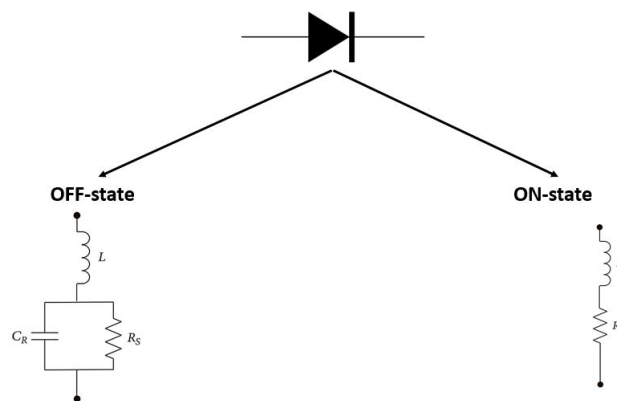

Figure 2. Diode and its equivalent circuits for different biasing voltages

The geometrical variation, i.e., insertion of the slots, will give rise to a second geometry, that has to be optimized at the same time with the main one. The *simultaneous* optimization of the two structures in Fig. 3, namely the main (initial) one and the second one with cuts represents the main novelty of the present work.

This work is organized as follows: Section II presents the proposed optimization method where HFSS with Matlab are working together. The validation of the method is proved by designing and optimizing the FSS that is described in Sec.III. The conclusions of this work are provided in Sec. IV.
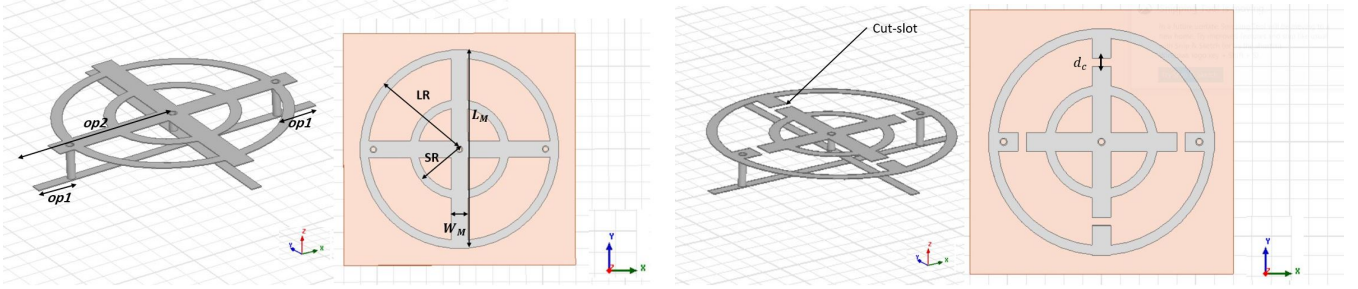
Figure 3. Initial geometry (left), geometry with the cuts (right)

2 Automated Random Optimization method for the FSS design

Optimization methods have got the attention of researchers in various radio frequency and microwave designs. These techniques are challenging with the nonlinear behavior and parasitic effects of designs and are aiming to achieve satisfied output performances with optimal solutions. Hence by employing these methods, more accurate outcomes can be obtained with respect to parametric analysis and the difficulties of simulation, modeling, and layout generation can be reduced. Therefore, the employed algorithm using the CAD tools must be computationally cost-effective and offering error-free reliable outcomes.

EDA tools are well adopted to the analysis; however, when the amount of data is increasing, the analysis by these software can be prohibitive from computational resources and time points of view; advanced analysis tools are required for solving the optimization problems. Numerical analyzers can assist the EDA tools to enhance the accuracy issues and to minimize the human interruptions. Matlab is one of the very successful software for analyzing large amount of data and able to do operations over the various functions. With the combination of EDA tool and numerical analyzer, here Matlab, advanced optimization environments can be created where optimization algorithms can be easily implemented ad applied. Among the various optimization methods mentioned in the introduction part, the RO method is preferred as it is flexible to be executed in EDA tool and can be performed easily with numerical analyzers.

The RO, as its name suggests, is the process of randomly iterating the design parameters up to achieving suitable values of them [14]. In this method, the design parameters are iterated, i.e., increased or decreased, randomly up to achieving desired output performance. Fabrication constrains, i.e. minimum distance between microstrip lines, or their minimum width, are also employed in the optimization process and passed to the electromagnetic (EM) simulations in the EDA tools.

For our problem consisting of the design of a tunable FSS, we employ random optimization (RO) method for simultaneously optimize the two configurations considering their constitutive design parameters aiming to achieve the suitable output performances for both of them. The applied method is performed in an automated environment where HFSS with Matlab are co-operating together [15] for optimizing the FSS without any human interruption. As described in [16], providing an automated environment can pave the way of researchers to get rid of any designer's experience and to easily deal with the challenging design problems. The algorithm in Fig. 4 presents the proposed optimization method for design the high performance FSS.

Once the initial geometry for both the main and cut-slot structures have been set, the automated environment is created where HFSS is working in the background and Matlab is handling and elaborating all the simulation results. Hence, the effort for preparing the data for optimizing the circuit is substantially reduced. Then the RO algorithm is applied where the design parameters are randomly iterated and the parameters are either increasing or decreasing automatically. This iteration loop is continued up to attaining the suitable output performances.

3 Practical FSS Design and Optimizations

This section presents the structure of designed FSS. Figure 1 illustrates the main structure of $D_u \times D_v = 14 \times 14$ mm built on FR-4 substrate ($\varepsilon_r = 4.3$ and $\tan \delta = 0.025$) with thickness of $h1 = 1.58$ mm. Our proposed structure described in the previous section and shown in Fig. 3 (left) is characterized by the following *initial* dimensions: external radius of the large circle is LR= 6 mm, external radius of the small circle SR= 3 mm, width of the two rings $w = 0.5$ mm. Each of the two bias microstrip lines have the same width ($W_M = 1$ mm) and length ($L_M = 12$ mm).

The three via-holes serves connecting the main structure to the biasing lines. These later are reported in the inset of the figure. First via-hole is located on the left side of the structure $op1 = 1.8$ mm (this distance is measured from the edge of the FSS), and the second one is placed in the center of the FSS $op2 = 7$ mm. The third one has the same behavior as the first one but in order to keep the symmetric structure it is created on the right of the structure with the same distance of $op1$. Use of this redundancy
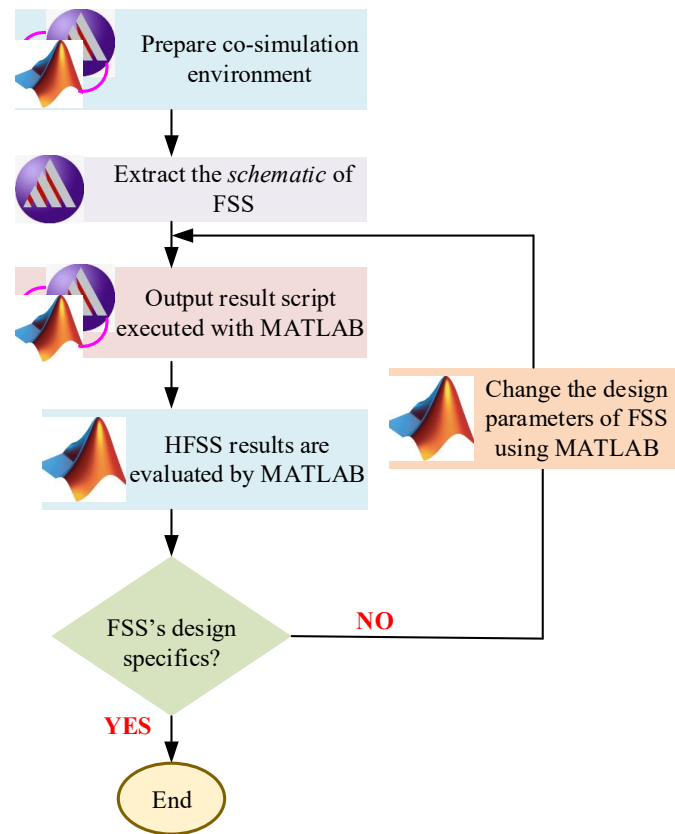
Figure 4. Proposed automated RO algorithm for optimizing FSS.

aims to reduce symmetry breaking, hence asymmetric answer of the circuit. Figure 3 illustrates the connection of via-holes to the biasing microstrip lines present for both the main and cut-slot structures. The reported values for the parameters refer to the initial design before applying the optimization process.

Figure 5 shows the results in terms of transmission coefficient (TC) for initial main structure for both TE (denoting E field parallel to *x* axis) and TM incidences (E field parallel to *x* axis); results for both the initial and optimized configurations are proposed. The initial structure for the main design has two frequency bands of interest (-10 dB): the first one is from 6.7 GHz to 9.5 GHz (2.8 GHz) and the second one covers 800 MHz (11.7 GHz - 12.5 GHz). After applying the optimization, the first band does not noticeably change but there is an increase of the second bandwidth up to 2.2 GHz, and an up shift of its central frequency. For TM incidence, the bandwidth of initial design and optimized one is almost constant but a shift in frequency happens from 11.2 GHz to 12.9 GHz for initial and optimized structure, respectively.

Figure 3 (right) reports the structure with the cut-slots. The result for this configuration for both initial and optimized designs are shown in Fig. 6 for TE and TM incidences. Following the optimization, for TE incidence, first frequency band notch shifts from 5 GHz to 5.8 GHz but maintaining almost the same bandwidth. Also, the second frequency band exhibits a frequency shift toward higher values. For the TM case similar behaviour can be noticed.

Phase difference between the TCs for TE and TM incidences for both initial and optimized structures are shown in Fig. 7 and Fig. 8, respectively. The initial main structure (Fig. 5) exhibits a transmission of -34.6 dB for TE incidence at the frequency of 8.2 GHz. For TM incidence at this frequency the TC is -3.2 dB; the huge dynamics shows that our structure behaves like linear polarizer. The second notch happens at 12 GHz (-20 dB) for TE incidence while for TM incidence it occurs at 11.6 GHz (-32 dB). Also, TCs for TE and TM incidences have intersection points at 9.7 GHz and 11.9 GHz. As Fig. 7 shows, $\pm 90°$ phase difference happens at four frequencies, namely at 8.3 GHz, 10.8, 11.6 GHz and 11.9 GHz. At the frequency of 11.6 GHz TE incidence has -1.2 dB and TM case exhibits -5.6 dB transmission, while at 11.9 GHz the two TCs are equal. Hence we can conclude that the initial main structure shows a circular polarization at frequency 11.9 GHz.

Figure 8 reports the phase difference for the main structure after optimization. In this figure at four points the structure exhibits $\pm 90°$ phase difference, more precisely at 8.5 GHz, 10 GHz, 12.9 GHz and 13.53 GHz. For TE incidence the first notch is at 8.35 GHz which has -31 dB transmission, then at mentioned frequency TM incidence has -1.2 dB transmission. 5.3 GHz and 10 GHz illustrate the points which TE and TM incidence interacted with each other for optimized main structure. According
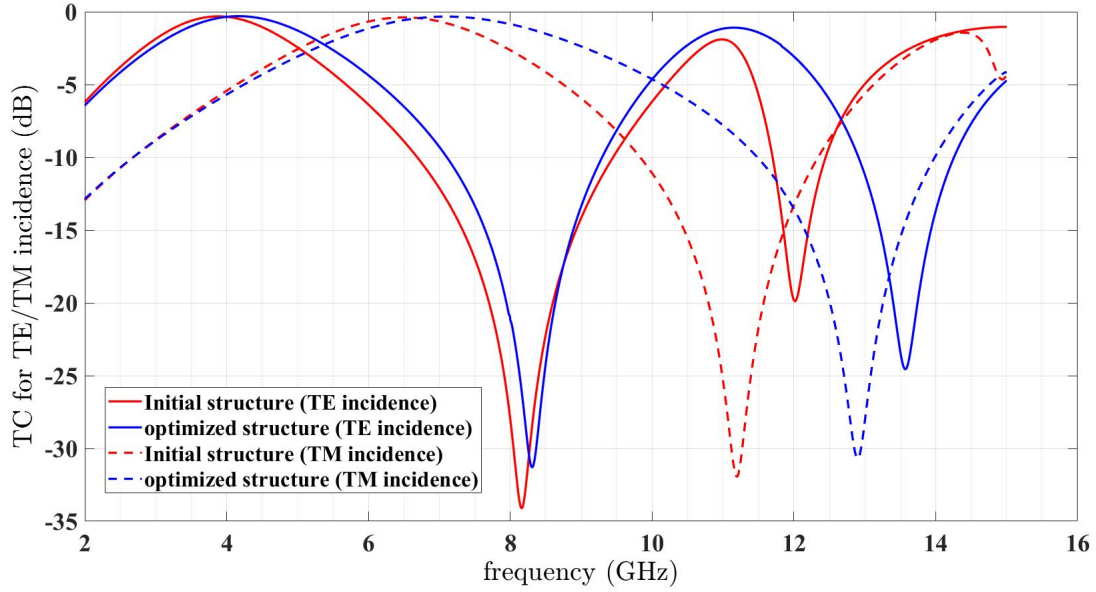
Figure 5. Transmission coefficient (TC) for initial and optimized main structure.
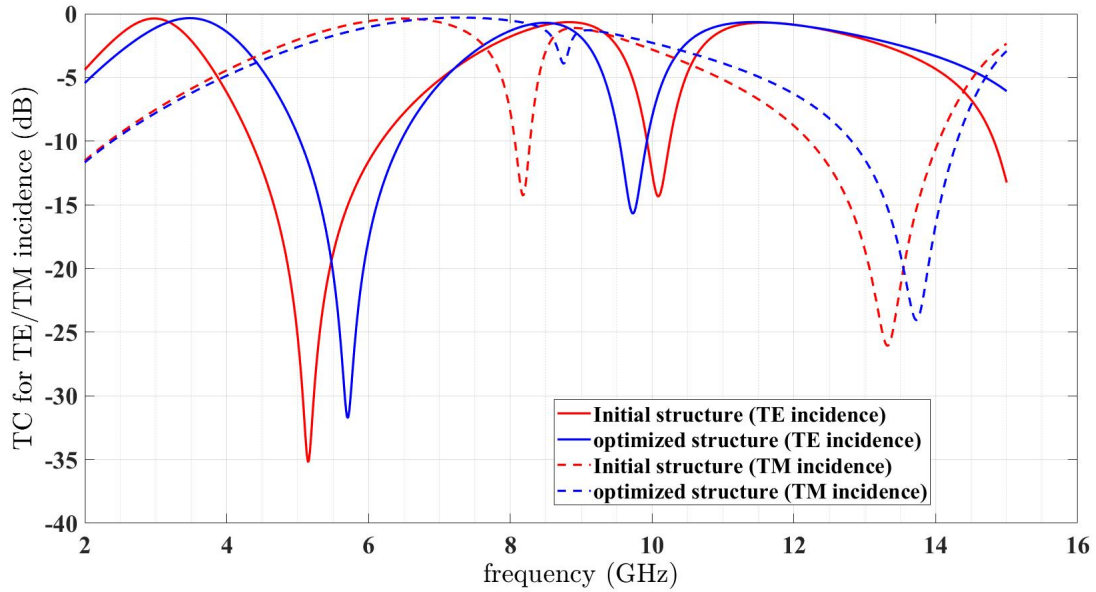

Figure 6. Transmission coefficient (TC) for initial and optimized cut-slot structure.

to Fig. 8 at 5.3 GHz our structure does not produce circular polarization, but at the frequency point of 10 GHz it shows that optimized FSS have circular polarization behavior.

Now we consider the structure with cut-slots; the results for TE and TM incidences in initial form and after optimization ares shown in Fig. 6. For TE incidence of initial structure with cut-slots notches are at 5.1 GHz and 10.1 GHz. At 5.1 GHz there is -35 dB in TE incidence transmission while for TM incidence it is -1.6 dB. The second notch is at 8.15 GHz and 10.1 GHz for TM and TE incidences, respectively. As Fig. 9 shows, this structure is not able to produce any circular polarization. The result for TE and TM incidences after optimization are represented in Fig. 6. Based on the results in this figure the first notch is at 5.9 GHz (-31.2 dB) for TE incidence, while for TM incidence the transmission is -1.2 dB. The second notch for TE happens at frequency of 9.8 GHz in which TM has 8.3 GHz. Based on the results in Fig. 9, our FSS structure for initial design with respect to cut-slot introduces 90° phase difference at four frequency points, namely 3.5 GHz, 5 GHz, 13.5 GHz and 14.8 GHz. By the means of optimization strategy as it is shown in Fig. 6 (blue curves) 5.8 GHz represents the first notch which is attenuated at -31 dB for TE, and -1.56 dB attenuation for TM incidence, respectively. The second notch for TE and TM happens at 9.7 GHz and 13.9 GHz. It is shown in Fig. 10 which at 13.9 GHz the FSS structure shows circular polarization. Also this figure represents four points for ±90° phase difference, namely at 4.1 GHz, 5.6 GHz, 13.9 GHz and 14.65 GHz.

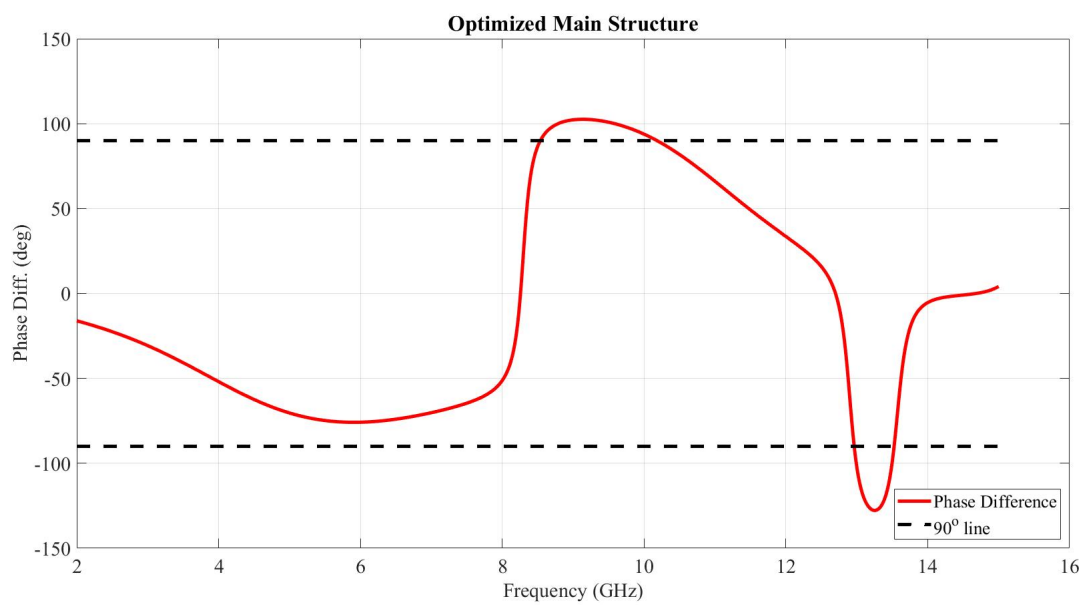**Figure 7.** Phase difference for initial main design.

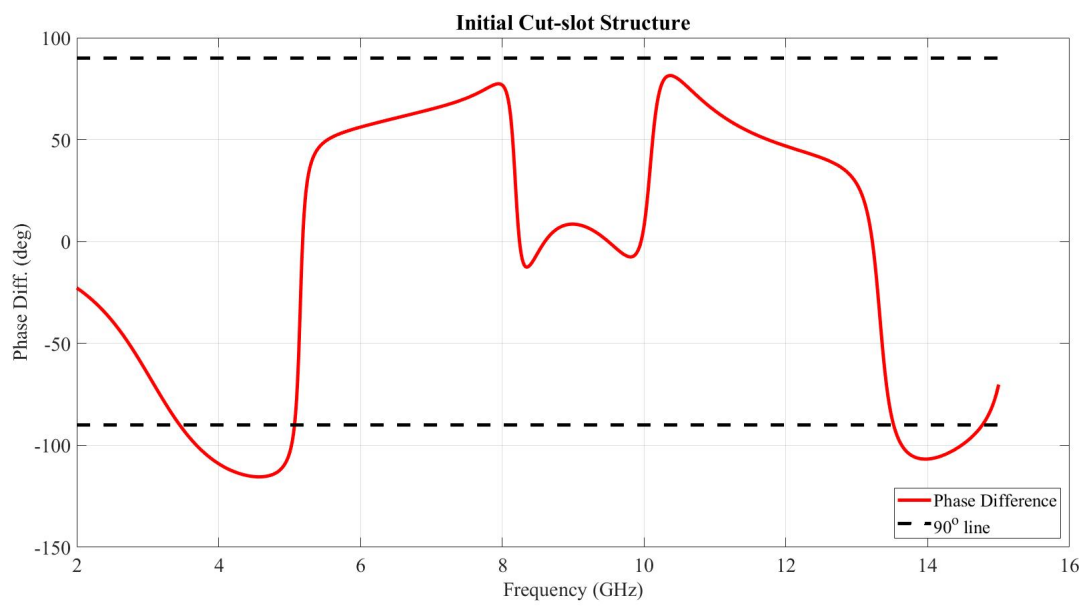**Figure 8.** Phase difference for optimized main design.

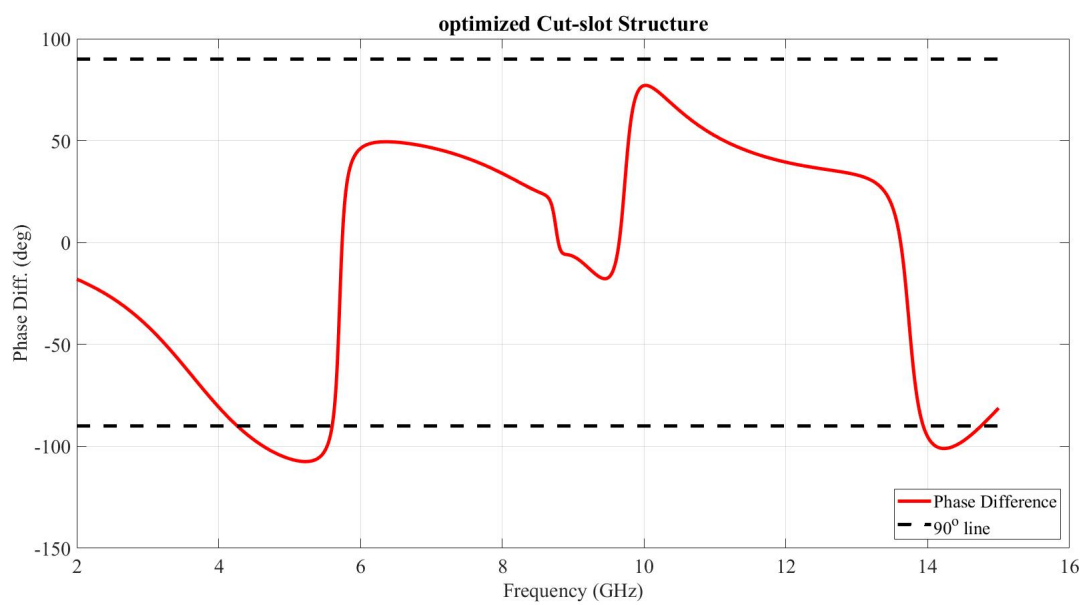**Figure 9.** Phase difference for initial cut-slot design.

Figure 10. Phase difference for optimized cut-slot design.

4 Effects of the inclusion of diodes in the FSS: study of their presence by equivalent lumped element circuit model

This section of the paper reports the results of the studies on the effect of diodes used in FSS to make our structure tunable. Figure 2 illustrates the equivalent circuit of diode for different biasing voltages. The behavior of FSSs is investigated by implementing the equivalent lumped element model of the diodes in this structure. Results for 4 identical diodes in the 4 slots for both initial and optimized structure are reported in Fig. 11 and Fig. 12, respectively. Comparison of these figures with Figs. 5 and 6 allows concluding that the results with the diodes inserted in the structure are similar to the unloaded configurations. This confirms the validity of the used models.
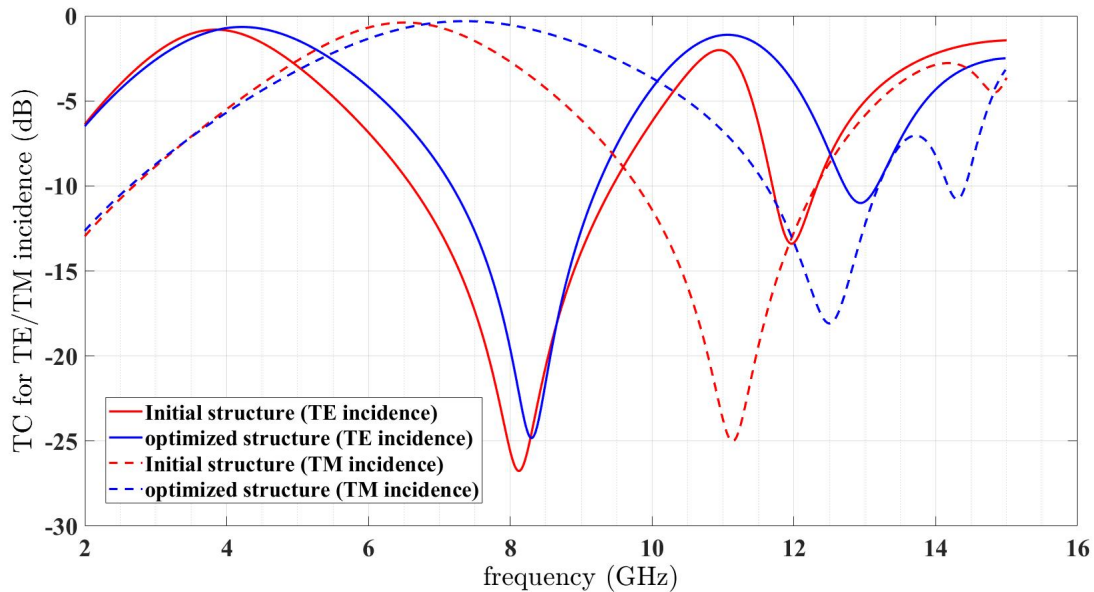

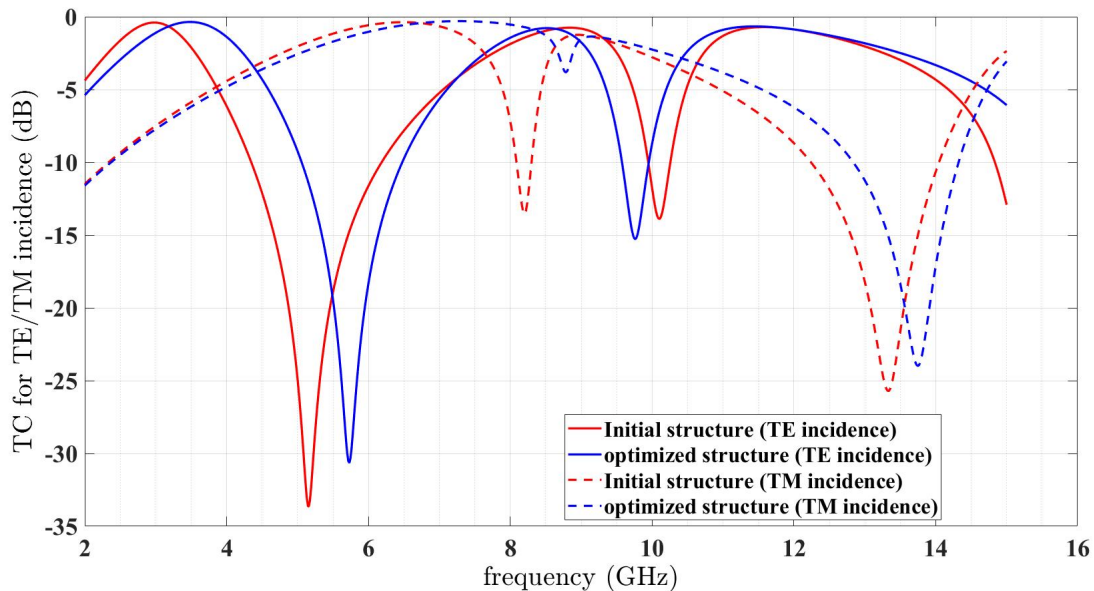**Figure 11.** ON-state diode for initial and optimized structures.

Figure 12. OFF-state diode for initial and optimized structures.

For FSS design in ON-state condition (initial structure) first frequency bands is at 3 GHz of bandwidth with −26.5 dB notch. Also, the second notch is at 12 GHz for TE and 11 GHz for TM incidence. By considering the optimization, in TE incidence the first notch frequency moves to 8.2 GHz with −25 dB transmission. But, for the second frequency band notches for TE and TM become closer which occur at 12.3 GHz and 12.4 GHz for TM and TE incidence, respectively.

In OFF-state condition of used diodes, as it is illustrated in Fig. 12, the first notch of the initial structure in TE incidence is at

5.4 GHz that moves to 5.8 GHz for the optimized one, 9.8 GHz and 10 GHz are the frequency points for the second notches for optimized and initial, respectively. As regards TM incidence, both initial and optimized cut-slot FSS have frequency notches at 13.65 GHz and 13.9 GHz.

5 Conclusion

In this work, we study the implementation of the RO method in an automated environment where HFSS and Matlab are collaborating together. The presented method is used in designing and optimizing a tunable FSS, based on two equivalent states of the involved diodes, which paves the way of designers for not challenging with huge amount of data. The FSS design is provided in HFSS and Matlab handles the optimization in order to find the suitable dimensions of the FSS geometry. From application point of view, comparison between the initial design and optimized one for both TE and TM incidences have been presented for the initial and diodes loaded configurations. Frequency bands for polarization converters have been identified: frequency bands exhibiting transmission of purely linear and/or circular polarized field have been identified.

References

[1] S. Ghosh and K. V. Srivastava, "A dual-band tunable frequency selective surface with independent wideband tuning," *IEEE Antennas and Wireless Propagation Letters*, vol. 19, no. 10, pp. 1808–1812, 2020.

[2] T. Gombor and J. Pávó, "Numerically efficient modeling of frequency selective surfaces in broad frequency range," *IEEE Transactions on Magnetics*, vol. 51, no. 3, pp. 1–4, 2015.

[3] A. O. Boryssenko, S. M. Gillette, and M. Y. Koledintseva, "Nonlinear loss model in absorptive-type ferrite frequency-selective limiters," *IEEE Transactions on Microwave Theory and Techniques*, vol. 67, no. 12, pp. 4871–4880, 2019.

[4] A. Ludvig-Osipov and B. L. G. Jonsson, "Evaluation of the electric polarizability for planar frequency-selective arrays," *IEEE Antennas and Wireless Propagation Letters*, vol. 17, no. 7, pp. 1158–1161, 2018.

[5] B. Döken and M. Kartal, "Easily optimizable dual-band frequency-selective surface design," *IEEE Antennas and Wireless Propagation Letters*, vol. 16, pp. 2979–2982, 2017.

[6] M. S. M. Mollaei, "Narrowband configurable polarization rotator using frequency selective surface based on circular substrate-integrated waveguide cavity," *IEEE Antennas and Wireless Propagation Letters*, vol. 16, pp. 1923–1926, 2017.

[7] M. A. Rodriguez Barrera and W. P. Carpes, "Bandwidth for the equivalent circuit model in square-loop frequency selective surfaces," *IEEE Transactions on Antennas and Propagation*, vol. 65, no. 11, pp. 5932–5939, 2017.

[8] S. Genovesi, R. Mittra, A. Monorchio, and G. Manara, "Particle swarm optimization for the design of frequency selective surfaces," *IEEE Antennas and Wireless Propagation Letters*, vol. 5, pp. 277–279, 2006.

[9] M. Zhao, X. Yu, Q. Wang, P. Kong, Y. He, L. Miao, and J. Jiang, "Novel absorber based on pixelated frequency selective surface using estimation of distribution algorithm," *IEEE Antennas and Wireless Propagation Letters*, vol. 14, pp. 1467–1470, 2015.

[10] R. Zhao, B. Gong, F. Xiao, C. He, and W. Zhu, "Circuit model analysis of switchable perfect absorption/reflection in an active frequency selective surface," *IEEE Access*, vol. 7, pp. 55 518–55 523, 2019.

[11] D. Z. Zhu, M. D. Gregory, P. L. Werner, and D. H. Werner, "Fabrication and characterization of multiband polarization independent 3-d-printed frequency selective structures with ultrawide fields of view," *IEEE Transactions on Antennas and Propagation*, vol. 66, no. 11, pp. 6096–6105, 2018.

[12] D. Z. Zhu, P. L. Werner, and D. H. Werner, "Design and optimization of 3-d frequency-selective surfaces based on a multiobjective lazy ant colony optimization algorithm," *IEEE Transactions on Antennas and Propagation*, vol. 65, no. 12, pp. 7137–7149, 2017.

[13] M. Kiani, M. Tayarani, A. Momeni, H. Rajabalipanah, and A. Abdolali, "Self-biased tri-state power-multiplexed digital metasurface operating at microwave frequencies," *Opt. Express*, vol. 28, no. 4, pp. 5410–5422, Feb 2020. [Online]. Available: http://www.opticsexpress.org/abstract.cfm?URI=oe-28-4-5410

[14] G. Xu, S. V. Hum, and G. V. Eleftheriades, "A technique for designing multilayer multistopband frequency selective surfaces," *IEEE Transactions on Antennas and Propagation*, vol. 66, no. 2, pp. 780–789, 2018.

[15] C. Jarufe, R. Rodriguez, V. Tapia, P. Astudillo, D. Monasterio, R. Molina, F. P. Mena, N. Reyes, and L. Bronfman, "Optimized corrugated tapered slot antenna for mm-wave applications," *IEEE Transactions on Antennas and Propagation*, vol. 66, no. 3, pp. 1227–1235, 2018.

[16] L. Kouhalvandi, O. Ceylan, and H. B. Yagci, "Power amplifier design optimization with simultaneous cooperation of eda tool and numeric analyzer," in *2018 18th Mediterranean Microwave Symposium (MMS)*, 2018, pp. 202–205.